Structural and magnetic properties of ammonia-nitrided Y_2Fe_{17}

1999 J. Phys.: Condens. Matter 11 833

(http://iopscience.iop.org/0953-8984/11/3/022)

J. Phys.: Condens. Matter **11** (1999) 833–845. Printed in the UK PII: S0953-8984(99)96581-5

Structural and magnetic properties of ammonia-nitrided Y_2Fe_{17}

N X Shen†, J I Budnick†, W A Hines†, Y D Zhang†, D P Yang‡ and Y G Duan§

† Department of Physics and Institute of Materials Science, University of Connecticut, Storrs, CT 06269, USA
‡ Department of Physics, College of the Holy Cross, Worcester, MA 01610, USA
§ Department of Chemistry, University of Connecticut, Storrs, CT 06269, USA

Received 6 August 1998, in final form 26 October 1998

Abstract. In order to make a comparison with N_2-gas nitrogenation, the structural and magnetic properties of ammonia-nitrided $Y_2Fe_{17}N_x$ were investigated by a combination of x-ray diffraction, magnetization and nuclear magnetic resonance. It was found that by using NH_3, the nitrogenation temperature and/or time are greatly reduced, and nominal N concentrations $0 \leqslant x \leqslant 6.3$ are obtainable. For lower N content, $x \leqslant 3.3$, a two-phase (nitrided + unnitrided) configuration exists in the sample particles. The unnitrided phase is completely suppressed for $x \geqslant 3.8$; however, an amorphous-like phase appears for $x \geqslant 5.6$. The average value for the magnetic moment per Fe atom initially increases with the N content, reaching a maximum for $x \approx 4$ before decreasing. The magnetic anisotropy, which arises solely from the Fe sublattice, is reduced for higher N content, but is still basal planar. These results indicate that the microscopic structure of the nitrided phase in ammonia-nitrided $Y_2Fe_{17}N_x$ is different from that in the same material prepared by N_2-gas nitrogenation. Evidence is provided for the existence of more than three, most likely four, nitrogen atoms per formula unit in the nitrided phase when $x > 3$.

1. Introduction

Recently, much research effort has been made to improve the hard magnetic properties of the binary R_2Fe_{17} (R = rare-earth) intermetallic compounds by interstitial and/or substitutional modifications of the 2:17 structure. This effort was stimulated by the discovery that introducing interstitial nitrogen or carbon atoms by means of a gas–solid reaction resulted in an increase in the Curie temperature and saturation magnetization; and, in the case of $Sm_2Fe_{17}N_x$, changed the anisotropy from basal planar to uniaxial [1, 2]. A volume expansion, which can be as much as 6% compared to the binary compounds, is also observed in all of the interstitial compounds. It is noteworthy that $Sm_2Fe_{17}N_x$ possesses better hard magnetic properties than those of $Nd_2Fe_{14}B$ and is a promising candidate for permanent magnet applications [3].

Nitrogenation of the R_2Fe_{17} compounds to produce $R_2Fe_{17}N_x$ involves a diffusion process which is initiated by exposing the parent material to a nitrogen-containing atmosphere at elevated temperature. Generally speaking, samples prepared by nitrogenation with N_2 gas have compositions with $x < 3$, while NH_3 gas yields considerably higher N content. The latter requires 'milder' nitrogenation conditions, i.e., lower reaction temperature and shorter reaction time. Nearly all of the reports in the literature concerning the use of NH_3-gas nitrogenation involve the preparation of $Sm_2Fe_{17}N_x$ [1, 2, 4–7]; however, reports for the single compositions $Y_2Fe_{17}N_{2.3}$ [1] and $Nd_2Fe_{17}N_{4.5}$ [8] also appear. In the work reported here, a combined

0953-8984/99/030833+13$19.50

x-ray diffraction (XRD), magnetization and nuclear magnetic resonance (NMR) study of the structural and magnetic properties for the ammonia-nitrided $Y_2Fe_{17}N_x$ system (nominal N content $0 \leqslant x \leqslant 6.3$) is presented. For this system, the transition-metal yttrium takes the place of the rare-earth element; however, yttrium has a very small magnetic moment and makes no contribution to the magnetic anisotropy, thus enabling the behaviour of the Fe sublattice to be isolated. The results presented here shed light on: (1) the location, distribution and concentration of the N atoms, (2) the magnetic properties and behaviour and (3) the resulting final structure or phases of the material.

2. Experimental apparatus and procedure

The parent Y_2Fe_{17} ingot was prepared by arc melting using Y and Fe starting materials with a purity of 99.95%. Since yttrium has a relatively low boiling point and high vapour pressure, an additional amount of yttrium ($\leqslant$5% by weight) was added to the starting materials to compensate for the loss during arc melting. The polycrystalline parent Y_2Fe_{17} ingot was annealed in vacuum at approximately 900 °C for one week, ground into a powder and passed through sieves to obtain particle diameters in the three ranges: <20 μm, 20 to 25 μm and 25 to 32 μm.

The NH_3-gas nitrogenation was carried out in a chamber which was first evacuated (typically 10^{-6} Torr) and flushed with high purity nitrogen gas several times. The parent Y_2Fe_{17} fine powders were exposed to NH_3 gas with a gauge pressure of 0.14 to 0.20 atm in the chamber while being heated to temperatures in excess of 300 °C for various times. At the conclusion of the gas–solid reaction, the chamber was cooled down to 200 °C and evacuated. It is known that nitrogenation with NH_3 will also introduce H atoms into the 2:17 lattice. The 200 °C vacuum annealing process was continued for 2 to 3 hours in order to remove the hydrogen from the sample powder. Although the vast majority of H atoms were removed by the annealing process, a trace amount of residual hydrogen always remained as observed in the NMR spectra (see below). The nominal nitrogen content was calculated by weighing the sample before and after the nitrogenation process. The particle size, gas pressure, reaction temperature and reaction time are all crucial factors for determining the nitrogen content (see table 1).

Table 1. $Y_2Fe_{17}N_x$ prepared by NH_3-gas nitrogenation of Y_2Fe_{17}.

Particle size (μm)	Temperature (°C)	Time (min)	N content
20 to 25	310	30	1.3
25 to 32	330	30	1.6
25 to 32	350	30	2.3
20 to 25	350	50	3.3
<20	350	60	3.8
25 to 32	350	360	4.1
25 to 32	380	180	4.6
20 to 25	350	270	5.6
<20	350	360	6.3

All XRD powder patterns were obtained by employing Cu Kα radiation and a Philips x-ray diffractometer which was equipped with a single-crystal monochromator. The diffraction intensity was recorded as a function of 2θ, the angle between the incident and the diffraction direction, using a home-made computer interface. The XRD patterns were characteristic of those for the Y_2Fe_{17} compound, with a mixture of the hexagonal (Th_2Ni_{17}-type) and

rhombohedral (Th_2Zn_{17}-type) structures. The patterns for both structures can be indexed on hexagonal unit cells, and only differ in their stacking sequence along the *c*-direction, which is ABAB... for the hexagonal structure and ABCABC... for the rhombohedral structure. The *a* and *c* lattice constants were obtained by performing a least squares fit to the diffraction peak 2θ-values.

In order to observe the saturation moment and magnetic anisotropy, samples consisting of fine powders were aligned at room temperature in a DC field of 16 kOe, and then fixed in epoxy resin. Y_2Fe_{17} is an easy-plane material with the easy plane being essentially isotropic. However, an alignment can still be achieved in a DC magnetic field with the *c*-axes of the fine magnetic particles being randomly distributed perpendicular to the field. Magnetization (magnetic moment per unit mass) isotherms $M(H)$ were obtained at 10 K for magnetic fields up to 55 kOe using a Quantum Design SQUID magnetometer. The magnetization was measured in two directions, i.e. magnetic field both parallel and perpendicular to the sample alignment direction. Before every measurement, the sample was completely demagnetized such that the magnetization curve obtained was the initial curve.

The zero-field spin-echo NMR spectra were collected at liquid helium temperatures using a phase-coherent pulse spectrometer over the frequency range 5 to 60 MHz which included resonances from the ^{1}H and ^{89}Y nuclei. Details of the methodology of NMR in magnetically ordered materials, including the experimental procedure and data acquisition, are available elsewhere [9].

3. Experimental results, analysis and discussion

Table 1 lists the nitrogenation conditions and the resulting nitrogen concentrations for the ammonia-nitrided $Y_2Fe_{17}N_x$ (nominal N content $0 \leqslant x \leqslant 6.3$) samples studied in this work. The results reported here are consistent with the work of Iriyama *et al* [2] on $Sm_2Fe_{17}N_x$ ($0 \leqslant x \leqslant 6.6$) samples prepared by nitrogenation with a mixture of NH_3 and H_2 gases. They used somewhat larger particle size (20–106 μm), along with slightly higher temperature (420–495°C), higher NH_3 partial pressure (0.35–0.45 atm) and longer reaction time (up to 8 hours). Compared to N_2-gas nitrogenation, it was found that the use of NH_3 gas to produce $Y_2Fe_{17}N_x$: (1) yields N content greater than 3.0 and (2) requires milder nitrogenation conditions, i.e. lower reaction temperature and/or shorter reaction time.

3.1. X-ray diffraction

Figure 1 shows the XRD patterns for the ammonia-nitrided $Y_2Fe_{17}N_x$ powder samples with $x = 0$, 1.6, 3.8 and 6.3. For the unnitrided parent Y_2Fe_{17} sample (figure 1(*a*)), the XRD pattern is typical of that for the Y_2Fe_{17} compound. It is well known that the Y_2Fe_{17} compound crystallizes into either the Th_2Ni_{17}-like hexagonal structure, Th_2Zn_{17}-like rhombohedral structure or, in most cases, a mixture of these structures [10]. Of the eight peaks labelled *hkl* in figure 1(*a*), six appear for both the hexagonal structure (without parenthesis) and the rhombohedral structure (with parenthesis and the appropriate 2:3 ratio for *l*). The structure is uniquely identified by the characteristic peaks for each type, i.e. the 203 hexagonal peak at $2\theta = 41.0°$ and (024) rhombohedral peak at $2\theta = 37.8°$. There is a trace of the 123 hexagonal peak (not labelled) at $2\theta = 46.5°$. Also, there is a hexagonal 114 peak and a rhombohedral (215) peak; however, they both occur near $2\theta = 49.1°$ and are hard to distinguish. In this work, the set of diffraction peaks labelled in figure 1(*a*) for the parent Y_2Fe_{17} powder sample (with the mixture of the hexagonal and rhombohedral structures) will be designated as characterizing the 'unnitrided phase'. In figure 1(*b*) for the $Y_2Fe_{17}N_{1.6}$ sample, two sets of diffraction peaks exist

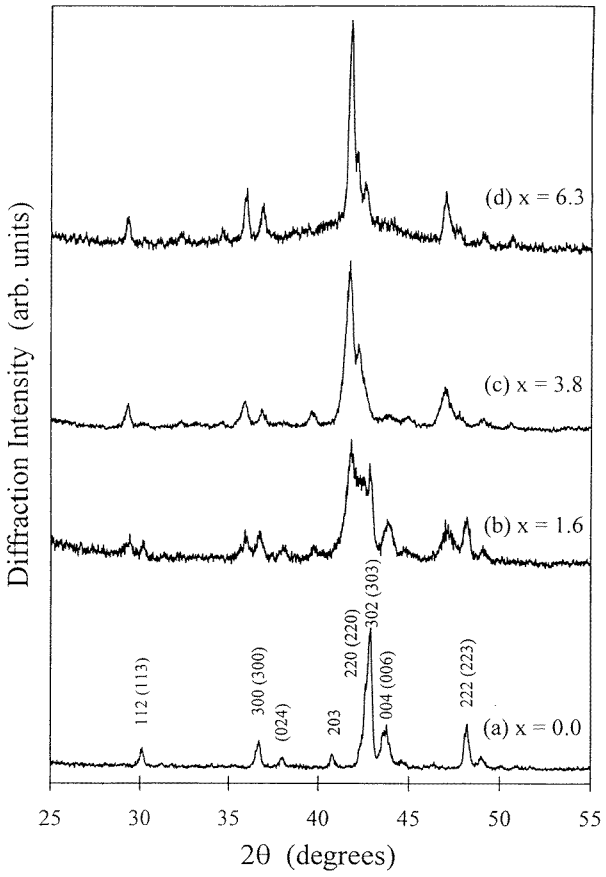

Figure 1. X-ray diffraction powder patterns for ammonia-nitrided $Y_2Fe_{17}N_x$: (*a*) $x = 0$, unnitrided parent phase (*hkl* without parenthesis—hexagonal structure, *hkl* with parenthesis—rhombohedral structure), (*b*) $x = 1.6$, both unnitrided and nitrided phases present, (*c*) $x = 3.8$, nitrided phase only, and (*d*) $x = 6.3$, nitrided phase with some amorphous phase background.

which partially overlap, and which clearly indicate the presence of a two-phase structure. One set, which is consistent with smaller lattice constants, corresponds to the unnitrided Y_2Fe_{17} phase, while the second set, which is consistent with larger lattice constants, corresponds to a $Y_2Fe_{17}N_x$ 'nitrided phase' (again, both phases having a mixture of the hexagonal and rhombohedral structures). As seen in table 1, the particle size of the parent Y_2Fe_{17} powder used for the $Y_2Fe_{17}N_{1.6}$ sample was 25–32 μm. Using a shell–core model for the sample particles, with the nitrided region being the shell and the unnitrided region being the core, along with a consideration of the penetration depth for Cu Kα radiation in Y_2Fe_{17} (approximately 5 μm), one would not expect to observe the diffraction peaks from the unnitrided phase. The two-phase shell–core structure was supported by a recent XRD study on $Y_2Fe_{17}N_{1.7}$ prepared by N_2-gas nitrogenation [11]. A sample of $Y_2Fe_{17}N_{1.7}$ consisting 32–37 μm particles initially showed only one set of peaks which was characteristic of the nitrided phase ($Y_2Fe_{17}N_x$). However, when the sample powder was ground to smaller particle size, a second set of peaks characteristic of the unnitrided Y_2Fe_{17} phase appeared. In the case of $Y_2Fe_{17}N_{1.6}$ prepared by NH_3-gas nitrogenation presented here, the initial appearance of both sets of peaks is due to the

presence of hydrogen during nitrogenation. When the ammonia decomposes at approximately 300 °C, the released hydrogen, whether in atomic or molecular form, will immediately diffuse into the interstitial sites of the lattice and react with the parent Y_2Fe_{17} powder. Hydrogen decrepitation occurs in which microcracks are produced and, ultimately, the particle size is reduced [4]. This process has been used effectively in industry.

Evidence for the two-phase configuration was also found in the XRD patterns for $Y_2Fe_{17}N_{2.3}$ and $Y_2Fe_{17}N_{3.3}$, which were both similar to the XRD pattern for $Y_2Fe_{17}N_{1.6}$, except that the intensity of the nitrided peaks increased at the expense of the unnitrided peaks. Figure 1(*c*) shows the XRD pattern for the $Y_2Fe_{17}N_{3.8}$ sample which is characterized by only the one set of diffraction peaks for the nitrided phase. This was also the case for $Y_2Fe_{17}N_{4.1}$ and $Y_2Fe_{17}N_{4.6}$. The XRD patterns for $Y_2Fe_{17}N_{5.6}$ and $Y_2Fe_{17}N_{6.3}$ (shown in figure 1(*d*)), while still exhibiting only one set of diffraction peaks characteristic of the nitrided phase, also show a broad background which indicates the existence of some type of amorphous-like phase for larger N content. The amorphous-like feature can be seen to appear under the three closely spaced peaks (220 (220), 302 (303) and 004 (006)) near $2\theta \approx 42^\circ$. Iriyama *et al* [2] have observed a similar feature in the XRD patterns obtained for ammonia-nitrided $Sm_2Fe_{17}N_x$ with $x \geqslant 5.9$. A Mössbauer study by Li *et al* [5] revealed that the amorphous-like phase in $Sm_2Fe_{17}N_x$ is paramagnetic.

The a and c lattice constants relevant to the hexagonal unit cells were obtained from a least squares fit of 10 hexagonal (rhombohedral) peaks. Figure 2 shows the lattice constant a versus the N content x for ammonia-nitrided $Y_2Fe_{17}N_x$ ($0 \leqslant x \leqslant 6.3$). The values obtained from the hexagonal peaks are consistent with those from the rhombohedral peaks within experimental error. Also, the expansion of the lattice along the a-axes due to nitrogenation is apparent, as well as the two-phase configuration for $x = 1.6$ and 2.3. (The unnitrided XRD peaks were not distinct enough to be fitted for $x = 3.3$.) Figure 3 shows the layer–layer distance L ($c/4$ for the hexagonal structure and $c/6$ for the rhombohedral structure) versus the N content for $Y_2Fe_{17}N_x$. Again, the expansion of the lattice along the c-axis due to nitrogenation is apparent. As the error bars are approximately the size of the symbols, the distinct jump between $x = 2.3$ and 3.3 is significant. As discussed below, this behaviour provides evidence for one additional N atom entering the 2:17 lattice per formula unit when $x > 3$. Finally, the volume per formula unit, V_{fu}, which characterizes both the unnitrided and nitrided phases,

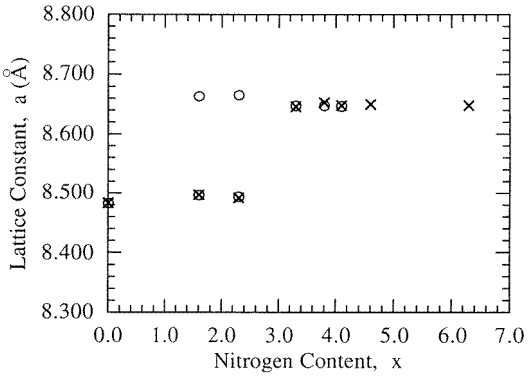

Figure 2. The lattice constant a (Å) versus the N content x for ammonia-nitrided $Y_2Fe_{17}N_x$ ($0 \leqslant x \leqslant 6.3$): open circles—fit to hexagonal structure, crosses—fit to rhombohedral structure. The error bars are approximately the size of the symbols. The unnitrided phase is observed for $0 \leqslant x \leqslant 3.3$ (although only fitted up to 2.3), while the nitrided phase is observed for $1.6 \leqslant x \leqslant 6.3$.

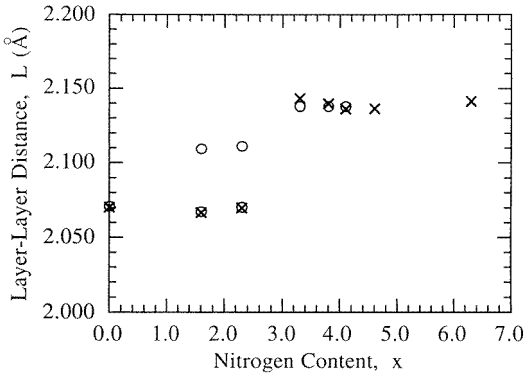

Figure 3. The layer–layer distance L (in Å) versus the N content x for ammonia-nitrided $Y_2Fe_{17}N_x$ ($0 \leqslant x \leqslant 6.3$), where L is $c/4$ for the hexagonal structure (open circles) and $c/6$ for the rhombohedral structure (crosses). The error bars are approximately the size of the symbols. The unnitrided phase is observed for $0 \leqslant x \leqslant 3.3$ (although only fitted up to 2.3), while the nitrided phase is observed for $1.6 \leqslant x \leqslant 6.3$.

Table 2. Ammonia-nitrided $Y_2Fe_{17}N_x$ crystallographic data.

Sample	a (Å)	$\Delta a/a$ (%)	L (Å)	$\Delta L/L$ (%)	V_{fu} (Å^3)	$\Delta V_{fu}/V_{fu}$ (%)
Y_2Fe_{17}[a]	8.483	0.0	2.071	0.0	258.1	0.0
$Y_2Fe_{17}N_{1.6}$[b]	8.664	2.1	2.110	1.9	274.3	6.3
$Y_2Fe_{17}N_{3.8}$[b]	8.651	2.0	2.139	3.3	277.2	7.4

[a] Unnitrided phase.
[b] Nitrided phase.

was calculated from the a and c lattice constants for $Y_2Fe_{17}N_x$ ($0 \leqslant x \leqslant 6.3$). Since the hexagonal structure has two formula units per unit cell volume whereas the rhombohedral structure has three, $V_{fu} = (a^2c\sin 60^\circ)/2$ for the former and $V_{fu} = (a^2c\sin 60^\circ)/3$ for the latter. It was found that the difference between the V_{fu} values for the two structures lies within experimental error. A description of the lattice expansion resulting from NH_3-gas nitrogenation is provided in table 2. The maximum N content that is obtainable in the 2:17 structure is still an open question. The hexagonal (rhombohedral) structure provides three octahedral 6h (9e) and six tetrahedral 12i (18g) interstitial sites per formula unit. It has been usually assumed that the N atoms occupy only the octahedral interstitial sites [12]; however, Jaswal *et al* [13] have pointed out the possibility of N atoms entering the tetrahedral interstitial sites. As listed in table 2, the lattice parameters for the nitrided phase in NH_3-gas prepared $Y_2Fe_{17}N_{1.6}$ (e.g. $\Delta V_{fu}/V_{fu} = 6.3\%$) are very similar to those reported previously for the nitrided phase in N_2-gas prepared samples, and for which an upper limit of three N atoms per formula unit is generally accepted [12]. On the other hand, the lattice parameters for the nitrided phase in NH_3-gas prepared $Y_2Fe_{17}N_{3.8}$ (e.g. $\Delta V_{fu}/V_{fu} = 7.4\%$) are consistent with the work of Brennan *et al* [14] on NH_3-gas prepared $Sm_2Fe_{17}N_{3.9}$. In their work, they provide evidence to suggest the existence of N atoms in sites other than the octahedral interstitial sites and that the number of N atoms in the nitrided phase is closer to four. They report an approximate value for the lattice expansion of 2.1% per N atom.

Finally, for the ammonia-nitrided $Y_2Fe_{17}N_x$ samples reported here, the XRD patterns showed no trace of any peaks due to Fe_4N, Fe_3N or YN. There is a slight indication of a peak at 44.7° which is due to bcc α-Fe; however, as can be seen in figure 1(*a*), this apparently came

in with the parent powder and was not due to the ammonia nitrogenation treatment. The XRD measurements alone cannot totally rule out the possibility of phase separation in the lower N content samples, particularly if the second phase(s) form(s) with nanoscale dimensions. However, in contrast to N_2-gas prepared samples, where the bcc α-Fe precipitates increase with the N content and can be as large as 10% [15], the amount of bcc α-Fe precipitation with NH_3 preparation is clearly reduced.

3.2. Magnetization

Figures 4(*a*)–4(*h*) show the magnetization M (in emu g^{-1}) versus the magnetic field H (in kOe) measured at 10 K for eight of the magnetically aligned fine-particle samples of ammonia-nitrided $Y_2Fe_{17}N_x$ ($0 \leqslant x \leqslant 6.3$). The '$\|$' notation indicates a direction of the magnetic

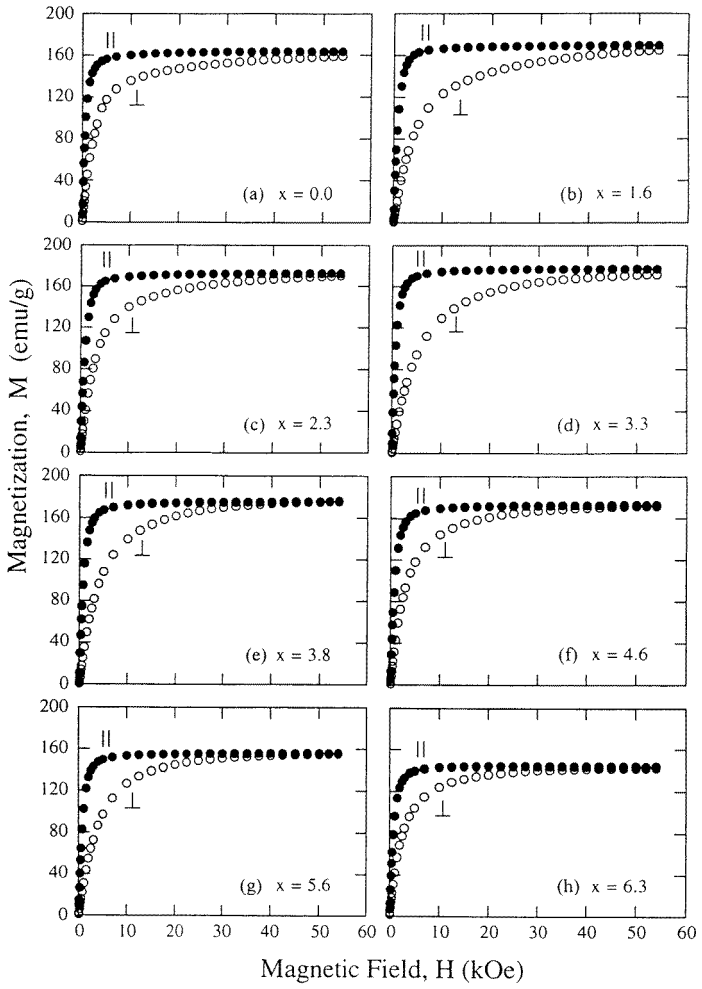

Figure 4. Magnetization M (in emu g^{-1}) versus magnetic field H (in kOe) measured at 10 K for magnetically aligned fine-particle samples of ammonia-nitrided $Y_2Fe_{17}N_x$ ($0 \leqslant x \leqslant 6.3$): '$\|$' indicates applied field parallel to alignment direction and '$\perp$' indicates applied field perpendicular to alignment direction.

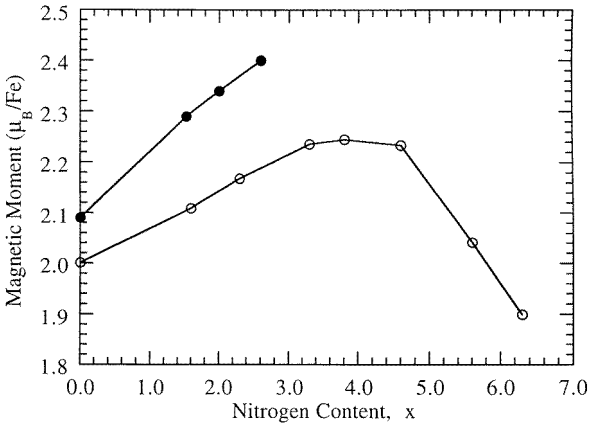

Figure 5. The average magnetic moment per Fe atom (in μ_B) versus the N content x for $Y_2Fe_{17}N_x$ ($0 \leqslant x \leqslant 6.3$): open circles—nitrided with NH_3 gas (this work), closed circles—nitrided with N_2 gas [17].

field parallel to the alignment direction and the '$\perp$' notation indicates a direction of the magnetic field perpendicular to the alignment direction. Values of the saturation magnetization M_s were obtained by fitting the various magnetization curves above 15 kOe to the form $M(H) = M_s - (A/H) - (B/H^2)$, and converted to Bohr magnetons per formula unit (μ_B fu^{-1}) using M_s (μ_B fu^{-1}) $= M_s$(emu g^{-1}) $\times W/5585$, where W is the formula unit weight (in g). In order to calculate an average value for the magnetic moment per Fe atom, $\langle \mu_{Fe} \rangle$, the moment value for yttrium is assumed to be -0.40 μ_B and independent of the N content [16]. Also, if it is assumed that nitrogen has no appreciable moment, $\langle \mu_{Fe} \rangle$ can then be obtained from the measured saturation magnetization using

$$\langle \mu_{Fe} \rangle = \frac{M_s(\mu_B \text{ fu}^{-1}) + 2 \times 0.40}{17}. \tag{1}$$

Figure 5 shows $\langle \mu_{Fe} \rangle$ versus the N content x for the $Y_2Fe_{17}N_x$ samples in this work (open circles). It can be seen that $\langle \mu_{Fe} \rangle$ initially increases with increasing N content, obtains a maximum for $x \approx 4$, and then decreases. The behaviour of $\langle \mu_{Fe} \rangle$ shown in figure 5 should be considered in the light of two competing effects, one being the exchange interaction between two Fe atoms and the other being the chemical bonding between an Fe atom and its neighbouring N atoms. The insertion of N expands the lattice and, hence, changes the Fe–Fe exchange interactions which results in an increase in the average Fe moment. The increase in $\langle \mu_{Fe} \rangle$ up to $x \approx 4$ is likely to be a consequence of the lattice expansion in the nitrided phase along with the growth of the nitrided phase at the expense of the unnitrided phase. However, the chemical bonding between Fe and its N neighbours will eventually decrease the average Fe moment for large N content. Also, the appearance of a paramagnetic amorphous-like phase for large N content will result in a reduced value for the average Fe moment. The magnetic moment behaviour illustrated in figure 5 suggests that there exist more than three N atoms in the nitrided phase for N content $x > 3$. For comparison, the values obtained for $\langle \mu_{Fe} \rangle$ from N_2-prepared $Y_2Fe_{17}N_x$ samples have been included (solid circles) [17]. Comparing the two curves, the difference between the initial values for $x = 0$ is most likely due to a small difference in the stoichiometry of the parent ingots. It is well known that the hexagonal Y_2Fe_{17} phase can exist over a finite range of composition [10]. What is more significant, however, is the difference in the initial slope for the two curves with NH_3-prepared samples having a

smaller incremental change in $\langle \mu_{Fe} \rangle$ per N atom. If the difference between the two curves is attributed to the presence of bcc α-Fe in the N_2-prepared samples, this would require that the amount of bcc α-Fe in $Y_2Fe_{17}N_{2.6}$ be approximately 40%. As described above, previous NMR measurements carried out on N_2-prepared $Y_2Fe_{17}N_x$ indicate that the amount of bcc α-Fe does increase with the N content; however, it does not exceed 10% [15]. Consequently, it is concluded that the difference between the NH_3-prepared samples and the N_2-prepared samples for a given nominal composition lies in the difference in the microscopic nature of the nitrided phase for the two types, i.e. location and concentration of the N atoms. The NMR results described below address this issue further on a microscopic level.

Finally, values of the anisotropy field H_a (defined as $-2K_1/M_s$, where K_1 is the second-order anisotropy constant) were extracted from the magnetization data in figure 4 using a simple model described by Li *et al* [18], which is directly applicable to magnetically aligned fine-particle samples. In their model, the magnetic process within one single domain is considered with the total energy (magnetic field and anisotropy) being minimized thereby obtaining an expression which contains the angles that the magnetization and the magnetic field make with the c-axis. The expression is then solved numerically. From these results, the value of H_a can be obtained from experimental data by plotting the reduced magnetization (defined as the ratio of the perpendicular and parallel magnetization values) as a function of the applied magnetic field. In particular, H_a is calculated from the magnetic field value for which $(M_\perp/M_\parallel) = 0.935$. The magnetic field value is then corrected for demagnetization effects by using a demagnetization factor of $N \sim 1/10$ for the fixed fine-powder samples. Figure 6 shows H_a versus the N content for $Y_2Fe_{17}N_x$. As indicated above for $Y_2Fe_{17}N_x$, with Y taking the place of the rare-earth element, the only contribution to the anisotropy is from the Fe sublattice. What is important to note here is that using NH_3-gas nitrogenation to obtain $Y_2Fe_{17}N_x$ with nominal N content up to $x = 6.3$ results in a reduction of H_a by approximately one-half. However, the anisotropy, which is easy plane for Y_2Fe_{17}, clearly does not change over to easy axis.

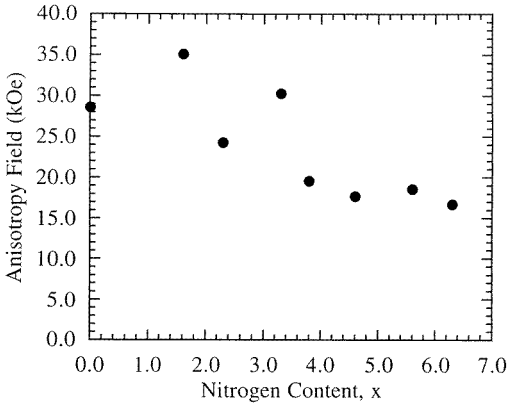

Figure 6. The anisotropy field H_a (in kOe) versus the N content x for ammonia-nitrided $Y_2Fe_{17}N_x$ ($0 \leqslant x \leqslant 6.3$). Although H_a decreases for large N content, the anisotropy remains basal plane.

3.3. Nuclear magnetic resonance

In order to obtain a clearer picture concerning the microscopic structure, zero-field spin-echo NMR spectra were obtained from the ammonia-nitrided $Y_2Fe_{17}N_x$ samples at liquid-helium temperatures over the frequency range 5 to 60 MHz. Since the hydrogen and nitrogen atoms

have no moment, while the yttrium atoms have a very small moment (magnitude $\approx 0.40\ \mu_B$), the hyperfine field at these sites is essentially that transferred from the nearest neighbour Fe atoms. Consequently, the observation of the resonance peaks from the ^{1}H, ^{14}N and/or ^{89}Y nuclei provides information concerning the local atomic environment.

In this section, a detailed comparison will be made between samples of $Y_2Fe_{17}N_x$ prepared by: (a) N_2-gas nitrogenation studied previously and (b) NH_3-gas nitrogenation reported here. In previous work on N_2-gas prepared $Y_2Fe_{17}N_x$ with nominal N content $0 \leqslant x \leqslant 2.8$ (see [19]), the sample particles were described as being 'two phase' with a nitrided outer shell and an unnitrided inner core. The ^{89}Y spectra obtained from $Y_2Fe_{17}N_x$ were characterized by four resonance peaks located at 42.5, 36.5, 29.5 and 26.5 MHz, and designated Y(0), Y(1), Y(2) and Y(3), respectively. In this notation, the Y(0) peak was attributed to the unnitrided Y_2Fe_{17} phase, as the Y atoms have no N atoms in the neighbouring interstitial sites. The three satellite lines Y(1), Y(2) and Y(3) were attributed to the nitrided $Y_2Fe_{17}N_x$ phase, and the number in the parenthesis indicates the number of N atoms in neighbouring interstitial sites, i.e., Y(1) and Y(2) have one and two N atoms in neighbouring octahedral interstitial sites, respectively, and Y(3) has two N atoms in neighbouring octahedral interstitial sites and one N atom in a neighbouring tetrahedral interstitial site. It was found that as the nitrogenation process progressed, the relative intensity ratio between the three satellite peaks remains constant (with the Y(2) peak being dominant), and the intensity of the three-satellite-peak combination increased at the expense of the Y(0) peak. The Y(0) peak, which characterizes the unnitrided Y_2Fe_{17} phase, completely disappeared when the N content reached $x \approx 2.6$ to 2.8. Consequently, in the two-phase model, the nitrogenation process proceeds with the growth of the outer nitrided shell at the expense of the inner unnitrided core; however, the microscopic nature of the nitrided phase apparently does not change.

The ^{89}Y spectra obtained for the NH_3-prepared samples in this work showed considerable differences from those obtained from the N_2-prepared samples cited above, reflecting differences in the microscopic atomic structure. Figure 7 shows the NMR spectrum obtained from the ammonia-nitrided $Y_2Fe_{17}N_{1.6}$ sample at 1.3 K over the frequency range 25 to 47 MHz. There is a strong (unnitrided phase) Y(0) peak at 42.5 MHz; however, the (nitrided phase) three-satellite-peak combination does not appear. (The small peak near 36 MHz could possibly be a Y(1) peak; however, there is no trace of the Y(2) and Y(3) peaks. Also, it is possible that this small peak is due to a small number of H atoms which remain in the tetrahedral interstitial sites after the vacuum anneal process (see below).) It is very striking that the three-satellite-peak combination which characterizes the nitrided phase in $Y_2Fe_{17}N_x$ prepared by N_2-gas nitrogenation does not appear for any of the ammonia-nitrided samples in this work. The intensity of the Y(0) peak for the ammonia-nitrided $Y_2Fe_{17}N_x$ samples did decrease with increasing N content; however, it was still observable for $x = 3.3$. This indicates the existence of some amount of unnitrided phase for nominal N content $x > 3$. Since the nominal N content was obtained by weighing the samples before and after nitrogenation, the value that is obtained reflects the product of the N content in the nitrided phase and the fraction of the sample particles that is the nitrided phase. Therefore, the above NMR result suggests that the nitrogen content in the nitrided phase exceeds three per formula unit for $x > 3$. This is consistent with the lattice expansion behaviour (see section 3.1) and the magnetic moment behaviour (see section 3.2).

Figure 8 shows the NMR spectrum obtained from the ammonia-nitrided $Y_2Fe_{17}N_{4.1}$ sample at 1.3 K. The Y(0) peak is absent as are the three satellite peaks. Instead, two weak and broad peaks appear at 36.0 and 47.0 MHz, with a frequency ratio of 1:1.31. These peaks characterize the ammonia-nitrided $Y_2Fe_{17}N_x$ samples for higher N content; they are more easily distinguished when the Y(0) peak is suppressed. Based on a very recent NMR study

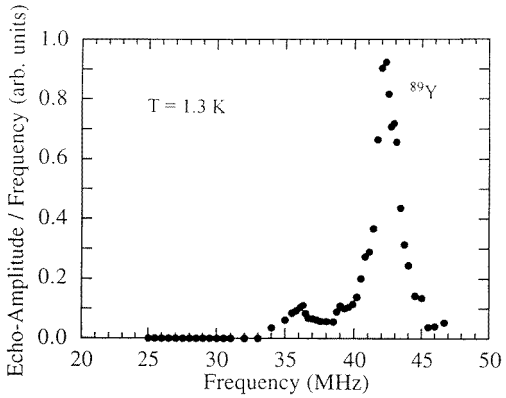

Figure 7. Zero-field spin-echo NMR spectrum obtained at 1.3 K for ammonia-nitrided $Y_2Fe_{17}N_{1.6}$. The large ^{89}Y peak at 42.5 MHz is characteristic of the unnitrided phase; the assignment of the small peak near 36 MHz is uncertain (see text).

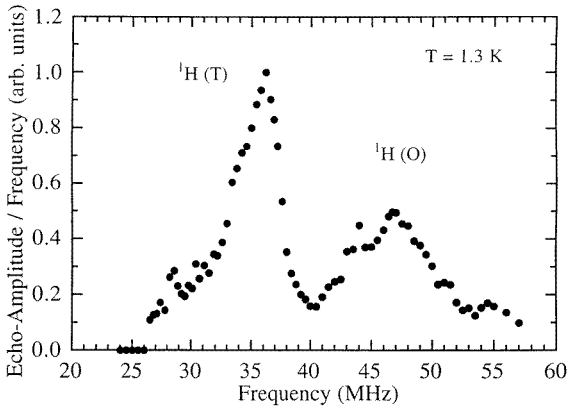

Figure 8. ^{1}H zero-field spin-echo NMR spectra obtained at 1.3 K for ammonia-nitrided $Y_2Fe_{17}N_{4.1}$: (O)—hydrogen atoms in the octahedral interstitial sites, (T)—hydrogen atoms in the tetrahedral interstitial sites.

of the nitri-hydride $Y_2Fe_{17}N_{2.8}H_5$, the peaks at 36.0 and 47.0 MHz are tentatively assigned to ^{1}H at the tetrahedral and octahedral interstitial sites, respectively [17]. Although all of the ammonia-nitrided $Y_2Fe_{17}N_x$ samples in this work were vacuum annealed at 200 °C for 2 to 3 hours before cooling to room temperature, it is apparent that a small amount of hydrogen still remained. It should be noted that in general the resonance from ^{1}H is extremely strong, and trace amounts of hydrogen in these samples would still be observable, particularly at 1.3 K. In the nitri-hydride work referred to above [17], hydrogen was loaded directly into a $Y_2Fe_{17}N_{2.8}$ powder sample (which was completely nitrided by using N_2 gas) and two ^{1}H peaks (at 37.5 and 51.0 MHz) appeared. By using a small correction for the difference in the average Fe moment value obtained with N_2-gas and NH_3-gas nitrogenation (see figure 5), the ^{1}H peak frequencies for $Y_2Fe_{17}N_{2.8}H_5$ match the peak frequencies above for ammonia-nitrided $Y_2Fe_{17}N_{4.1}$. Finally, it is noteworthy that Zhang *et al* [20] have observed ^{14}N peaks at 8.5 and 11.5 MHz (with a similar frequency ratio of 1:1.35) in N_2-prepared $Y_2Fe_{17}N_{2.6}$ which were attributed to N atoms in the tetrahedral and octahedral interstitial sites, respectively. Their

assignment was based on the relative intensities along with the fact that a tetrahedral site has two R and two Fe atoms as nearest neighbours while the octahedral site has two R and four Fe atoms as nearest neighbours.

From the ^{89}Y NMR study on the N_2-prepared $Y_2Fe_{17}N_x$ samples, it was observed (from the satellite peaks) that the ^{89}Y resonance peak shifts downward approximately 6.5 MHz for every N atom in a neighbouring octahedral interstitial site and 3.0 MHz for every N atom in a neighbouring tetrahedral interstitial site [19]. Based on these values and the indication that the nitrided phase in the NH_3-prepared $Y_2Fe_{17}N_x$ samples may contain more than three N atoms per formula unit, a search for the ^{89}Y resonance was carried out at 1.3 K and frequencies below 20 MHz for the $Y_2Fe_{17}N_{3.8}$ and $Y_2Fe_{17}N_{4.1}$ samples. Two peaks, which were broad and very weak, were observed at 11.5 and 17 MHz. The peak at 11.5 MHz could possibly be due to ^{14}N at the octahedral interstitial sites, although the corresponding peak at 8.5 MHz (tetrahedral sites) was not observed. The second peak at 17 MHz was tentatively assigned to ^{89}Y associated with the nitrided phase in these samples. At present, the reason(s) why the NMR peaks associated with the nitrided phase in the ammonia-nitrided samples are broader and weaker than expected is not understood in detail. Nevertheless, a consideration of all of the experimental results indicates a significant difference in the microscopic structure of the nitrided phase for N_2-gas and NH_3-gas nitrogenated $Y_2Fe_{17}N_x$.

4. Summary and conclusions

In order to compare 2:17 materials which have been nitrogenated using N_2 gas and NH_3 gas, a combined x-ray diffraction, magnetization and nuclear magnetic resonance study has been carried out on ammonia-nitrided $Y_2Fe_{17}N_x$ (nominal N content $0 \leqslant x \leqslant 6.3$). The replacement of the rare-earth constituent by yttrium enables the magnetic behaviour of the Fe sublattice to be isolated. It was found that the use of NH_3 gas in nitrogenation requires lower reaction temperature and shorter reaction time than with N_2 gas. Consequently, the precipitation of bcc α-Fe, which is unavoidable with the use of N_2 gas, is reduced. Furthermore, higher nominal N content x is obtainable using NH_3 gas; i.e., whereas $x \leqslant 2.8$ is typical using N_2 gas, $x = 6.3$ was obtained in this work and a report for $x = 8.0$ exists for $Sm_2Fe_{17}N_x$ [5]. However, the higher N content is accompanied by the appearance of an amorphous-like phase which makes the N content actually in the 2:17 crystalline structure somewhat uncertain. Also, along with the appearance of the amorphous-like phase is a degradation of the magnetic properties. Detailed XRD measurements of the ammonia-nitrided $Y_2Fe_{17}N_x$ system provide clear evidence for the two-phase, nitrided–unnitrided, shell–core configuration for $0 \leqslant x \leqslant 3.3$. For $x \geqslant 3.8$, only the peaks characteristic of the nitrided phase remain; however, a broad background appears for $x \geqslant 5.6$ indicating the existence of an amorphous-like phase for the higher N content samples. Values for the a and c lattice constants associated with the 2:17 hexagonal unit cells were obtained from a fit of the XRD peaks for both the nitrided and unnitrided phases. The c lattice constant (or layer–layer distance) for the nitrided phase shows a distinct jump between $x = 2.3$ and 3.3, which suggests that one additional site is being occupied by the N atoms. In particular, the measured lattice expansion of the nitrided phase is 6.3% for $x < 3$, which is similar to that obtained with N_2-gas prepared samples in which an upper limit of three N atoms per formula unit is generally accepted. However, for $x > 3$, a lattice expansion of 7.4% was observed, which is consistent with previous work on NH_3-gas prepared $Sm_2Fe_{17}N_x$, suggesting that the number of N atoms in the nitrided phase might be closer to four. The existence of more than three N atoms in the nitrided phase is also supported by the magnetic moment behaviour and NMR results. From magnetization measurements on magnetically aligned powders of ammonia-nitrided $Y_2Fe_{17}N_x$, values were obtained for the average magnetic moment per Fe

atom as well as the anisotropy field. The value for $\langle\mu_{Fe}\rangle$ increases with N content reaching a maximum for $x \approx 4$, and then decreases. The initial rate of increase of $\langle\mu_{Fe}\rangle$ with N content is less than that observed for N_2-prepared samples, and is attributed to differences in the nitrided phase (i.e. N location and concentration) for the two methods of nitrogenation. The anisotropy remains basal planar upon nitrogenation; however, it is reduced somewhat for higher N content. Finally, the NMR results clearly show that the $^{89}Y(0)$ line which characterizes the unnitrided (parent phase) exists for N content $x \leqslant 3.3$, and is not observable for $x \geqslant 3.8$. The $^{89}Y(1)$, $^{89}Y(2)$ and $^{89}Y(3)$ satellite peaks which occur for the nitrided phase in N_2-prepared $Y_2Fe_{17}N_x$ (and which are attributed to Y atoms with one, two and three N atoms as nearest neighbours) are not present for any of the NH_3-prepared samples in this work. This is especially significant for the samples with low N content (e.g. $Y_2Fe_{17}N_{1.6}$) which show a lattice expansion for the nitrided phase very similar to that for N_2-prepared samples. A pair of peaks are observed which can be attributed to a very small number of residual H atoms in both the tetrahedral and octahedral interstitial sites. The combined XRD, magnetization and NMR results from this work provide evidence for the existence of a nitrided phase which has more than three N atoms per formula unit, with a likely number being four. This is in contrast to N_2-gas nitrogenation which yields only two to three N atoms per formula unit. It is noteworthy that in previous work on ammonia-nitrided $Sm_2Fe_{17}N_x$, Brennan *et al* [14] have suggested that three of the (rhombohedral) octahedral interstitial 9e and one of the tetrahedral interstitial 18g sites are occupied by N atoms.

Acknowledgment

We gratefully acknowledge the support for this project from the National Science Foundation (grant No DMR-9705136).

References

[1] Coey J M D and Sun H 1990 *J. Magn. Magn. Mater.* **87** L251
[2] Iriyama T, Kobayashi K, Imaoka N, Fukuda T, Kato H and Nakagawa Y 1992 *IEEE Trans. Magn.* **28** 2326
[3] Li H S and Coey J M D 1991 *Handbook of Magnetic Materials* vol 6, ed K H J Buschow (Amsterdam: Elsevier) p 1
[4] Brennan S, Rao X L, Skomski R, Dempsey N and Coey J M D 1996 *J. Magn. Magn. Mater.* **157/158** 510
[5] Li H L, Takahashi K, Ujihira Y, Kobayashi K, Iriyama T and Konishi T 1994 *J. Mater. Sci.* **29** 6518
[6] Koenonger V, Uchida H H and Uchida H 1995 *J. Alloys Compounds* **222** 117
[7] Christodoulou C N and Komada N 1995 *J. Alloys Compounds* **222** 27
[8] Yan Q W, Zhang P L, Wei Y N, Sun K, Hu B P, Wang Y Z, Liu G C, Gau C and Cheng Y F 1993 *Phys. Rev.* B **48** 2878
[9] Zhang Y D, Budnick J I, Ford J C and Hines W A 1991 *J. Magn. Magn. Mater.* **100** 13 and references therein
[10] Shen N X, Zhang Y D, Budnick J I, Hines W A, Lyver R and Buschow K H J 1996 *Appl. Phys. Lett.* **69** 3194
[11] Zhang Y D, Budnick J I, Hines W A and Yang D P 1996 *J. Appl. Phys.* **79** 4596
[12] Ibberson R M, Moze O, Jacobs T H and Buschow K H J 1991 *J. Phys.: Condens. Matter* **3** 1219
[13] Jaswal S S, Yelon W B, Hadjipanayis G C, Wang Y Z and Sellmyer D J 1991 *Phys. Rev. Lett.* **67** 644
[14] Brennan S, Shomski R and Coey J M D 1994 *IEEE Trans. Magn.* **30** 571
[15] Zhang Y D, Yang D P, Budnick J I, Hines W A, Xu W Q, Shen N X, Pease D M, Fernando G W and Xiao T D 1995 *Scr. Metall. Mater.* **33** 1817
[16] Beuerle T and Fähnle M 1992 *J. Magn. Magn. Mater.* **110** L29
[17] Shen N X 1998 *PhD Thesis* University of Connecticut
[18] Li H S, Mohanty R C, Raman A, Grenier C G and Ferrell R E 1997 *J. Magn. Magn. Mater.* **166** 365
[19] Zhang Y D, Budnick J I, Yang D P, Fernando G W, Hines W A, Xiao T D and Manzur T 1995 *Phys. Rev.* B **51** 12 091
[20] Zhang Y D, Budnick J I, Hines W A, Shen N X, Xiao T D and Manzur T 1996 *J. Magn. Magn. Mater.* **145** L11